Accepted Manuscript

SmB_6 Nanoparticles: Synthesis, Valence States, and Magnetic Properties

Lihong Bao, Luomeng Chao, Yingjie Li, Ming Ming, B. Yibole, O. Tegus

PII: S0925-8388(15)30202-4
DOI: 10.1016/j.jallcom.2015.06.086
Reference: JALCOM 34428

To appear in: *Journal of Alloys and Compounds*

Received Date: 12 May 2015
Revised Date: 8 June 2015
Accepted Date: 10 June 2015

Abstract: Nanocrystalline SmB_6 particles were synthesized by the solid-state reaction of Sm_2O_3/$SmCl_3$ with $NaBH_4$ in the temperature range of 1000–1200 ^oC. The phase composition, grain morphology, microstructure and valence states of SmB_6 were investigated by using XRD, FESEM, HRTEM and XANES. It is interestingly found that the SmB_6 nanocrystalline particles with size of 50 nm are easily prepared by using $SmCl_3$ as raw material. The FFT patterns of HRTEM images reveal that the SmB_6 nanocrystalline particles have a high crystallinity with cubic structure. The XANES results show that the valence state of Sm is more likely Sm^{3+}. The magnetic measurement shows that the SmB_6 nanoparticles show paramagnetic behavior, but there is a small anomaly in the paramagnetic state. The present synthesis technique is novel and invaluable for developing highly crystallized SmB_6 nanoparticles.

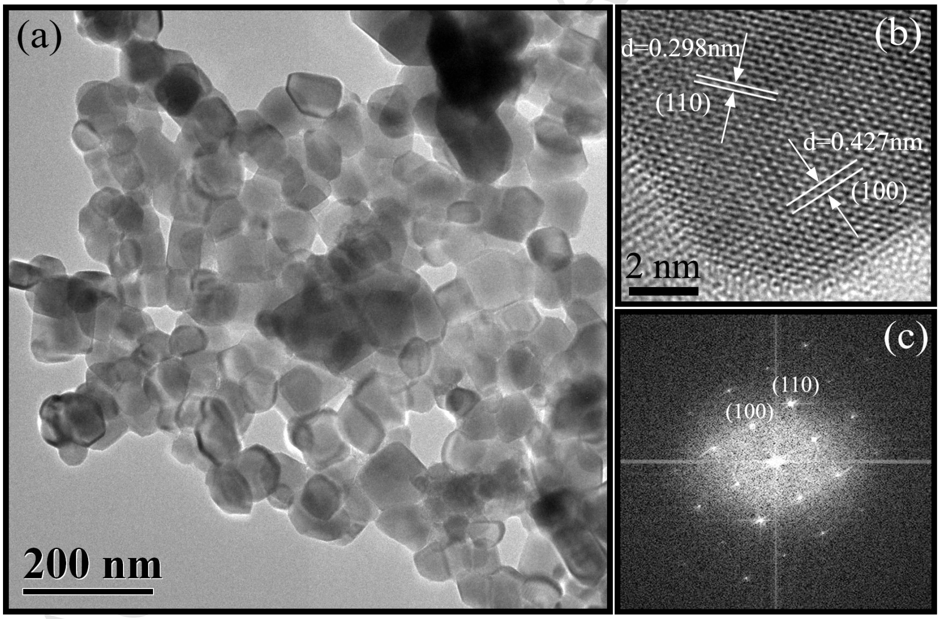

SmB_6 Nanoparticles: Synthesis, Valence States, and Magnetic Properties

Lihong Bao[a], Luomeng Chao[a,b], Yingjie Li[a], Ming Ming[a], B. Yibole[c], O. Tegus[a*]

[a]*Inner Mongolia Key Laboratory for Physics and Chemistry of Functional Materials, Inner Mongolia Normal University, Hohhot 010022, China*

[b]*Shenyang National Laboratory for Materials Science, Institute of Metal Research, Chinese Academy of Sciences, 72 Wenhua Road, Shenyang 110016, China*

[c] *Fundamental Aspects of Materials and Energy (FAME), Faculty of Applied Sciences, Delft University of Technology, Mekelweg 15, 2629 JB Delft, The Netherlands*

Nanocrystalline SmB_6 particles were synthesized by the solid-state reaction of $Sm_2O_3/SmCl_3$ with $NaBH_4$ in the temperature range of 1000–1200 ^oC. The phase composition, grain morphology, microstructure and valence states of SmB_6 were investigated by using XRD, FESEM, HRTEM and XANES. It is interestingly found that the SmB_6 nanocrystalline particles with size of 50 nm are easily prepared by using $SmCl_3$ as raw material. The FFT patterns of HRTEM images reveal that the SmB_6 nanocrystalline particles have a high crystallinity with cubic structure. The XANES results show that the valence state of Sm is more likely Sm^{3+}. The magnetic measurement shows that the SmB_6 nanoparticles show paramagnetic behavior, but there is a small anomaly in the paramagnetic state. The present synthesis technique is novel and invaluable for developing highly crystallized SmB_6 nanoparticles.

Key words: SmB_6, solid-state reaction, valence state
PACS number(s): 71.27.+a, 74.25.Jb, 75.70.Tj, 76.75.+i

1. Introduction

Rare-earth hexaborides (RB_6) with cubic CaB_6-type structure have been extensively investigated both theoretically and experimentally for decades [1-2]. Recently, several RB_6 nanowires such as LaB_6, CeB_6, PrB_6, NdB_6 and GdB_6 have been synthesized, and they are believed to be beneficial to developing field emission cathodes due to their low work function and a very sharp tip with diameters of less than hundred nanometers [3-7]. On the other hand, the optical absorption of RB_6 nanoparticles has also attracted much attention for the coexistence of high visible light transmission and strong near infrared absorption [8, 9]. These interesting optical absorption properties are well satisfied the demand for reducing solar heat for the windows of automotives and architectures, and have also potential applying for medical care [10-12]. More recently, the mixed valence SmB_6 as a multi-functional

* E-mail address: tegusph@imnu.edu.cn

hexaboride is considered the candidate material for topological Kondo insulators [13-15] and its optical absorption properties have become a hot research topic [16]. In addition, the SmB_6 have relatively lower work function of 3.11 eV and that makes it to be a potential thermionic emission material [17]. Therefore, there are great research prospects for further studying the SmB_6 intrinsic properties.

In general, there are many ways to prepare the SmB_6 materials. Hatnean *et al* have prepared the large sized and high quality SmB_6 single crystal by floating zone method [18]. SmB_6 nanowires are prepared by the liquid Sm (melting point of 1072 □) reacting with BCl_3 gas at a temperature of 1100 □ [19]. SmB_6 powders are prepared by a solid state reaction of Sm sources with B or B_4C at a high temperature of 1650 ^oC [20]. However, at this high reaction temperature, the stoichiometry of the products was hard to be well controlled due to the high volatilization nature of Sm element. In order to lower the reaction temperature, the Mg or I_2 as an effective catalyst was used to reduce the reaction temperature at a condition of autoclave [21-22].

In this paper, we report a simple and novel method for preparing the SmB_6 nanoparticles, using different Sm sources of $Sm_2O_3/SmCl_3$ reacting with $NaBH_4$ in a continuous evacuating process. The effects of different Sm sources on the phase composition, grain size, morphology, and the magnetic properties of SmB_6 nanoparticles were investigated by XRD, SEM, TEM, and magnetic measurements. As results the SmB_6 nanoparticles are more easily prepared by using $SmCl_3$ than Sm_2O_3 under same experimental condition. Meanwhile, present work provides evidence through XANES that the valence of Sm is about 2.88, indicating the surface state is dominant.

2. Experiment

$Sm_2O_3/SmCl_3$ (purity of 99.99%, Baotou Institute of Rare Earths) and $NaBH_4$ (purity of 99.0 %, Sigma-Alorich, USA) powders in a molar ratio of 1:12 and 1:6 were mixed in an agate mortar, respectively. Then the mixtures were pressed into pellet and reacted at a temperature between 1000~1200 ^oC for 2~4h. After reaction, the products were washed by hydrochloric acid and distilled water several times for removing the $SmBO_3$ impurity phase, which were formed during the reaction. The phase identification was examined by X-ray diffraction (Cu K_α radiation, Philips PW1830). The crystal surface morphology was characterized by field emission scanning electron microscope (FESEM: Hitachi SU-8010). The microstructure and EDS analysis are characterized by transmission electron microscopy (TEM: FEI-Tecnai F20 S-Twin 200 kV). The XANES measurement was carried out using synchrotron radiation at the BL-12A station of Photon Factory, Japan. The magnetic properties were measured by using SQUID magnetometer (Quantum Design MPMS 5XL).

3. **Results and discussion**

3.1. Phase Identification of SmB_6

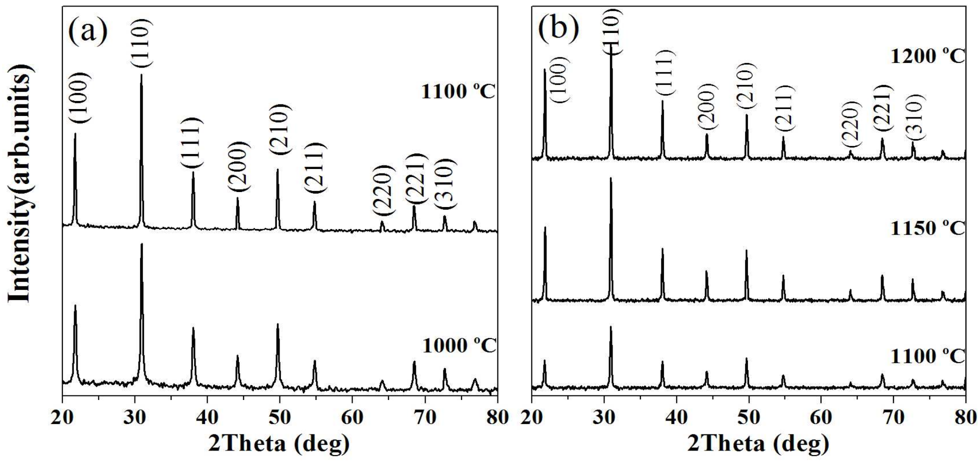

Fig. 1 XRD patterns of SmB_6 powder synthesized at different temperatures, (a) prepared Sm_2O_3 as raw material, (b) prepared $SmCl_3$ as raw material

Fig.1 (a) shows the XRD patterns of SmB_6 prepared at 1000 and 1100 ^oC for 4 h using Sm_2O_3 as raw material. It can be seen that all the diffraction peaks at these sintering temperatures can be assigned to the CaB_6-type single phase with space group of *Pm-3m* without any $SmBO_3$ impurity phase, confirming high purity of the synthesized products. For further increasing reaction temperature to 1150 ^oC, it is found that there is no powder product obtained after the reaction. This is probably caused by the high evaporation rate of Sm_2O_3 at high reaction temperature. By comparison with Fig.1 (b), it was found that in the case of using $SmCl_3$ as raw material, even the reaction temperature increases to 1150 and 1200 ^oC, we can obtain the single phase SmB_6. Its XRD patterns are well indexed and assigned to the parallel crystal plane of (100), (110), (111), (210) and (211), which is much different from the results of Sm_2O_3 as raw material. This means that it is easier to prepare SmB_6 nanoparticles using $SmCl_3$ as precursor than using Sm_2O_3 at same reaction temperature.

3.2. Micrograph and microstructure of SmB_6

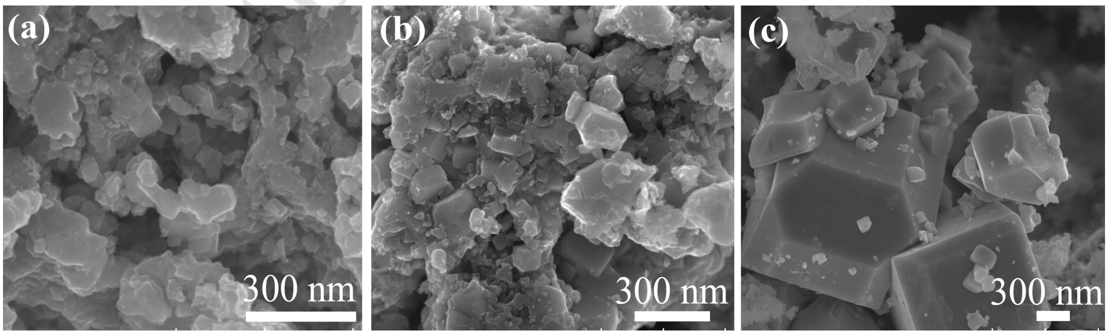

Fig. 2 FESEM images of SmB_6 prepared at different temperatures, using Sm_2O_3 as raw materials, (a) 1000 ^oC for 4 h, (b) 1100 ^oC for 4 h, (c) 1100 ^oC for 20 h

In order to better compare the grain sizes and typical shapes of SmB_6 products synthesized by using different raw materials, the field emission scanning electron microscopy (FESEM) images were shown in Fig. 2. It can be seen from Fig. 2 (a) that the SmB_6 prepared by using Sm_2O_3 at 1000 ^oC is mainly composed of a great deal of aggregated particles without any regular shapes. When the reaction temperature is 1100 ^oC, it is clearly seen from the Fig. 2(b) that a small amount of cubic shaped SmB_6 nanocrystals were observed, but there are some large grains with non-cubic morphology around them. For a prolonged reaction time of 20 h, as shown in Fig. 3(c), an obvious grain-growth behavior and the clear grain morphology of each individual particle were observed. The largest grain size is up to about 3 μm. This grain growth is probably caused by that the high specific surface and high diffusion coefficients of nanoparticles have caused the mass transport through lattice and grain boundaries.

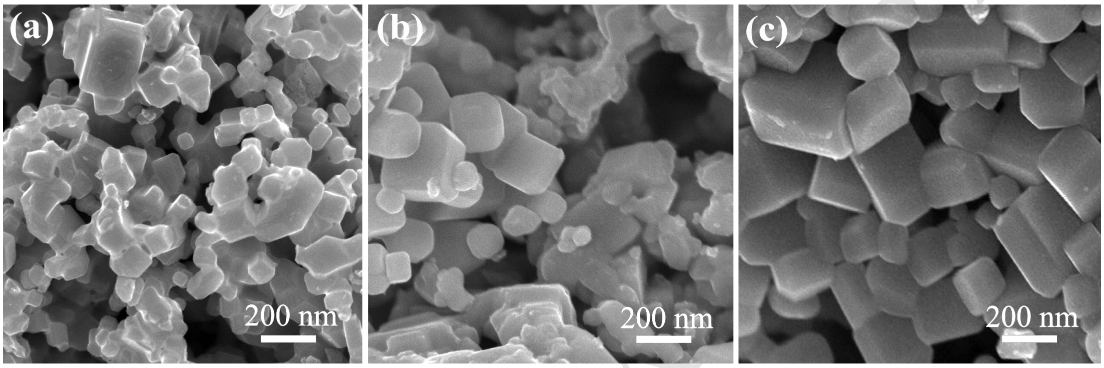

Fig. 3 FESEM images of SmB_6 prepared at different temperatures for 2 h, using $SmCl_3$ as raw material, (a) 1100 ^oC, (b) 1150 ^oC, (c) 1200 ^oC

Fig. 3 shows the FESEM image of SmB_6 nanoparticles prepared by $SmCl_3$ raw materials at different reaction temperatures. It can be found from Fig. 3 (a) there are a large number of small cubic grains initial formed with a mean size of 50 nm at 1100 ^oC, at the same time these crystals adhered together to show a less distributions. While the reaction temperature elevated to 1150 ^oC, some perfect nanocubes with a mean size of 100 nm formed and small amount of aggregated nanoparticles shown in Fig. 3 (b). Subsequently, with the increasing temperature to 1200 ^oC, all the crystals have crystallized into perfect cubic shape with average grain size of 200 nm and showed a good distribution, which is shown in Fig. 3(c). Comparing the FESEM observations of using Sm_2O_3 as raw material with $SmCl_3$, we have found the SmB_6 crystals prepared by $SmCl_3$ show an excellent crystallinity and more uniform distribution than Sm_2O_3. The reason is maybe the binding energy of Sm and O is stronger than that of Sm and Cl. Thus, $NaBH_4$ is easier to react with $SmCl_3$ rather than Sm_2O_3.

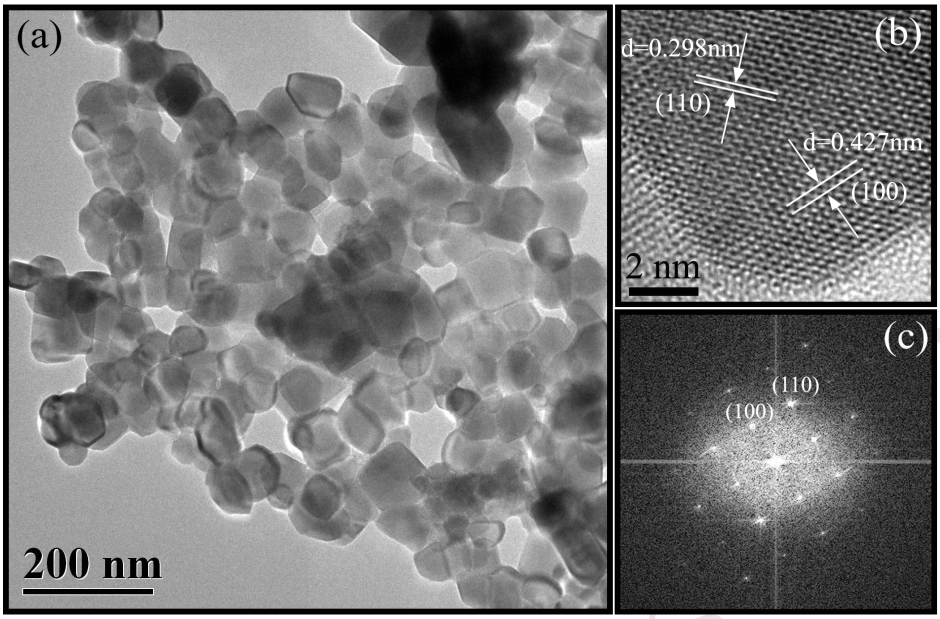

Fig. 4 (a) TEM analyses of SmB_6 nanocrystalline, **(b)** the HRTEM image (top right), **(c)** the indexing FFT patterns (down left).

For further study the microstructure of SmB_6 nanoparticles, transmission electron microscope (TEM) is used to characterize the grain morphology and crystallinity. A typical TEM image of SmB_6 nanoparticles prepared at 1100 ^{o}C is depicted in Fig. 4. It can be seen that the average grain size is around 40–50 nm, which is consistent with the SEM observation. The top right of HRTEM reveals the single crystalline nature of SmB_6 and the lattice fringes d = 0.427 nm and d = 0.298 nm, which agree well with the (100) and (110) crystal planes shown in Fig. 4(c), respectively. Up to now, Zhang *et al* [21] and Selvan *et al* [23] have successfully prepared the micron sized SmB_6 particle in a high pressure condition of autoclave. But in present work, this synthesis method shows an advantages of reaction process is easy controllable and the reaction does not require high pressure.

3.3. Valence states of SmB_6 nanoparticles

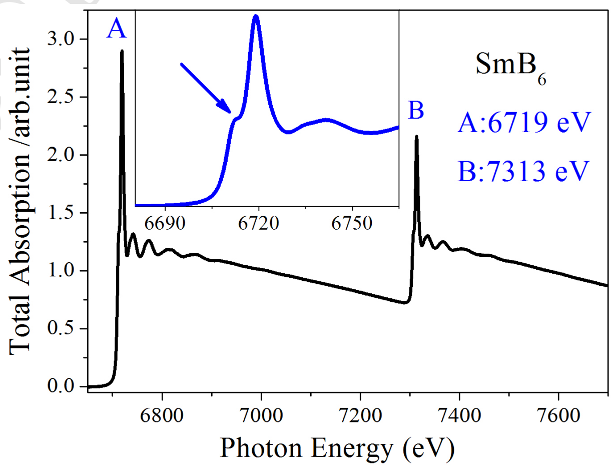

Fig. 5 (Color online) The total X-ray absorption spectra of SmB_6 nanoparticles against photon

energy at 295 K, The inset is XANES spectra around the Sm L_3 edge

Fig. 5 displays the total XANES spectra $\mu(E)$ around the Sm L_3 edge for SmB_6 nanoparticles at 295 K. It can be seen from the whole energy region that there is a couple of sharp white lines located at the position of 6719 eV and 7313 eV, which are corresponding to the absorption spectra of Sm L_3 and L_2 edge. From the upper side of enlarged image of peak A, it is clearly found there is a weak peak near it (marked in arrow), representing the Sm mixed valence states of trivalent (Sm^{2+}) and tetravalent (Sm^{3+}). The Sm^{2+} peak comes from the excitation from $2P_{3/2}$ to $5d$ orbital with final state $4f^6$ and the Sm^{3+} peak comes from the excitation from $2P_{3/2}$ to $5d$ orbital with final state $4f^5 5d^1$. This result is well agreement with the results [24].

In order to further study the valence state of SmB_6 in details, the Lorenzian function as following with an arctangent is applied to fit the absorption spectra:

$$\mu(E) = \frac{A_1(\Gamma/2)^2}{(E-E_1)^2+(\Gamma/2)^2} + \frac{A_2(\Gamma/2)^2}{(E-E_2)^2+(\Gamma/2)^2} + \left[0.5 + \frac{1}{\pi}\arctan\left(\frac{E-E_0}{\Gamma/2}\right)\right]$$

where E_1 and E_2 is the energy at which the transition from $2P_{3/2}$ to unoccupied $5d$ states occurs for trivalent and the tetravalent Sm, Γ is the core hole lifetime for the transition, A_1 and A_2 are the areas of the Lorenzian peaks. The arctangent function represents an infinite sum of Lorenzian functions characterized by the energy E_0 of the onset of the continuum. The parameters are summarized in Table 1 and the fitting curves are shown in Fig. 6. It is estimated the Sm valence from the areas A_1 and A_2 given in Table 1 is about 2.88, which is consistent with the results of Chazalviel *et al* [25].

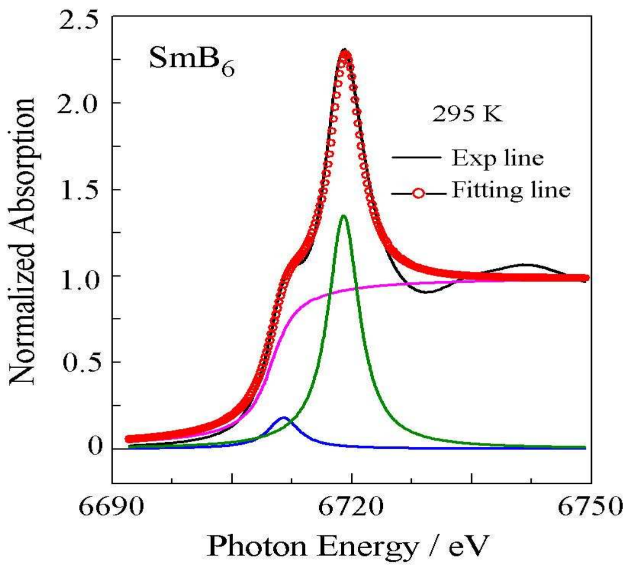

Fig. 6 (Color online) The fitting results of normalized Sm L_3 edge XANES spectra of SmB_6

Table 1 The parameters obtained from fitting the Sm $_{L3}$ edge XANES spectra to Lorenzian function

E_0 (eV)	E_1 (eV)	E_1-E_0 (eV)	E_2 (eV)	E_2-E_0 (eV)	Γ (eV)	A_1	A_2
6710	6711.5	1.5	6719	9	4.8	0.18	1.35

3.4 Magnetic properties of SmB_6

Fig.7 shows the magnetization as a function of temperature. The data were collected under zero-field-cooled (ZFC) and field-cooled (FC) conditions in an applied field of 10 mT. There is an opening between the ZFC and FC data, indicating irreversible or history dependent magnetism in SmB_6. A dome shaped magnetization curve is observed in the $M(T)$ data below 70 K, which does not show the typical behavior of paramagnet. The inset in Fig. 7 shows the full $M(H)$ loop of SmB_6, collected at 2.5 K. There is no observable hysteresis in the $M(H)$ loop. However, a clear deviation from a linear paramagnetic response is observed at low fields. These behaviors are almost same as those observed in bulk samples [26].

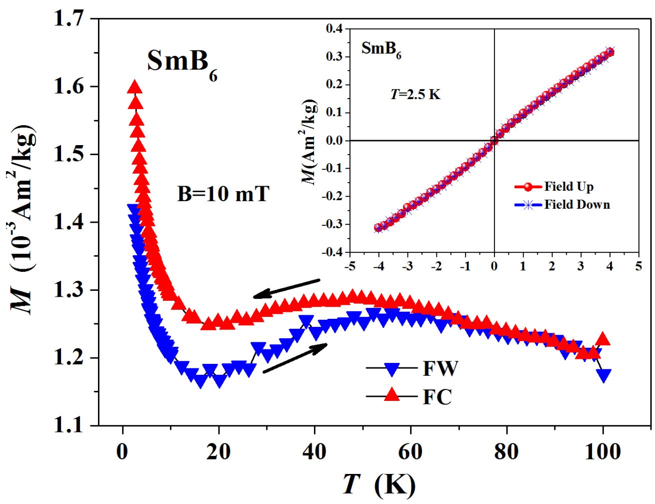

Fig. 7 (Color online) Temperature dependence of the magnetization of SmB_6 nanoparticles measured under ZFC and FC conditions in an applied field of 10 mT. Inset shows the full $M(H)$ loop of SmB_6 measured at 2.5 K.

3.5. Reaction mechanism of synthesis SmB_6

Based on the above mentioned experimental analysis, the $NaBH_4$ has played an important role for a reducing agent and as a boron source for whole synthesis procedure at the same time. Thus, at initial chemical reaction procedure, following reaction must be preceding at about 500 °C [27-28] regardless of Sm_2O_3 or $SmCl_3$ as raw materials as shown in Eq. (1).

$$NaBH_4\,(S) \rightarrow NaH(S) + BH_3\,(S) \quad (1)$$

At second step, Sm_2O_3 or $SmCl_3$ reacts with BH_3 to form the SmB_6 when the reaction temperature is higher than 1000 °C as described in Eq. (2), which is fully confirmed by the XRD analysis.

$$Sm_2O_3\ (S)\ \text{or}\ SmCl_3\ (S) + BH_3\ (S) \rightarrow SmB_6\ (S) + H_2\ (g) \qquad (2)$$

At last, the gaseous H_2 were removed by pumping and the impurity phase $SmBO_3$ was removed by hydrochloric acid washing.

4. Conclusions

In summary, a novel synthesis method for SmB_6 has been successfully demonstrated in present work. The advantages of the method are that the reaction process is easy controllable and the reaction does not require high pressure. It is easier to obtain the SmB_6 nanoparticles by using $SmCl_3$ as raw material than using Sm_2O_3. Furthermore, the grain size and morphology of SmB_6 nanocrystalline are very sensitive to the reaction temperature. The valence of Sm in the SmB_6 nanoparticles is 2.88, which is very close to the valence in the surface state. The magnetic properties of SmB_6 nanoparticles are same as those of bulk materials. The present preparation route is significantly important for developing new rare-earth nanomaterials with a wide range of possible applications.

Acknowledgements

This work is supported by Fundamental Research Open Project of Inner Mongolia (Grant No. 20130902), National Natural Science Foundation of China (No. 51302129) and Program for Young Talents of Science and Technology in Universities of Inner Mongolia (Grant No. NJYT-14-B03).

References

[1] J. M. Lafferty, J. Appl. Phys. 22 (1951) 299
[2] F. M. Hossain, D. P. Riley, G. E. Murch, Phys. Rev. B 72 (2005) 235101
[3] H. Zhang, Q. Zhang, G. P. Zhao, J. Tang, O. Zhou, L. C. Qin, Adv. Mater.18 (2006) 87
[4] C. Y. Zou, Y. M. Zhao, J. Q. Xu, J. Crystal Growth, 291 (2006) 112
[5] M. F. Chi, Y. M. Zhao, Q. H. Fan, W. Han, Ceram. Int. 40 (2014) 8921
[6] J. Q. Xu, G. H. Hou , T. Mori , H. Q. Li , Y. R. Wang , Y. Y. Chang ,Y. S. Luo , B. H. Yu , Y. Ma , T. Y. Zhai, Adv. Funct. Mater. 23(2013) 5038
[7] H. Zhang, Q. Zhang, G. P. Zhao, J. Tang, O. Zhou, L. C. Qin, J. Am. Chem. Soc. 127(2005)13120
[8] H. Takeda, H. Kuno, K. Adachi, J. Am. Ceram. Soc. 91(2008) 2897
[9] S. Schelm, G. B. Smith, Appl. Phys. Lett. 82 (2003) 4346
[10] B. H. Lai, D. H. Chen, Acta. Biomater 9(2013) 7556
[11] B. H. Lai, D. H. Chen, Acta. Biomater 9(2013) 7573
[12] M. C. Chen, K. W. Wang, D. H. Chen, M. H. Ling, C. Y. Liu, Acta. Biomater 13 (2015) 344
[13] P. Schlottmann, Phys. Rev. B 90(2014) 165127
[14] N. Heming, U. Treske, M. Knupfer, B. Büchner, D. S. Inosov, N. Y. Shitsevalova, V. B. Filipov, S. Krause, A. Koitzsch, Phys. Rev. B 90 (2014) 195128
[15] C. H. Min, P. Lutz, S. Fiedler, B. Y. Kang, B. K. Cho, H. D. Kim, H. Bentmann, F. Reinert, Phys. Rev. Lett. 112 (2014) 226402

[16] I. Batko, M. Batkova, Solid State Commun. 196 (2014) 18

[17] W. Waldhauser, C. Mitterer, J. Laimer, H. Stori, Surf. Coat. Technol. 98 (1998) 1315

[18] M. C. Hatnean, M. R. Lees, D. McK. Paul, G. Balakrishnan, Sci. Rep. 3 (2013) 3403

[19] J. Q. Xu, Y.M. Zhao, X. H. Ji, Q. Zhang, S. P. Lau, J. Phys. D 42 (2009) 135403

[20] J. Q. Xu, Y. M. Zhao, Z. D. Shi, C. Y. Zou, Q. W. Ding, J. Crystal Growth, 310 (2008) 3443

[21] M. F. Zhang, Y. Jia, G. G. Xu, P. F. Wang, X. Q. Wang, S. L. Xiong, X. J. Wang, Y. T. Qian, Eur. J. Inorg. Chem. (2010) 1289

[22]M. F. Zhang, X. Q. Wang, X. W. Zhang, P. F. Wang, S. L. Xiong, L. Shi, Y. T. Qian, J. Solid State Chem. 182 (2009) 3098

[23]R. K. Selvan, I. Genish, I. Perelshtein, Jose M. C. Moreno, A. Gedanken, J.Phys. Chem.C 112(2008)1795

[24]S. Gabani, K. Flachbart, J. Bednarcik, E. Welter, V. Filipov, N. Shitsevalova, Acta. Physica Polonica A. 126 (2014) 338

[25] J. N. Chazalviel, M. Campagna, G. K. Wertheim, P. H. Schmidt, Phys. Rev. B 14 (1976) 4586

[26] P. K. Biswas, Z. Salman, T. Neupert, E. Morenzoni, E. Pomjakushina, F. von Rohr, K. Conder, G. Balakrishnan, M. Ciomaga Hatnean, M. R. Lees, D. McK. Paul, A. Schilling, C. Baines, H. Luetkens, R. Khasanov, and A. Amato, Phys. Rev. B 89 (2014) 161107(R) J. H.

[27] Ma, J. Li, G. X. Li, Y. G. Tian, J. Zhang, J. F. Wu, J. Y. Zheng, H. M. Zhuang, T.H. Pan, Mater. Res. Bull. 42 (2007) 982

[28] Y. F. Yuan, L. Zhang, L. M. Liang, K. He, R. Liu, G. H. Min, Ceram. Int. 37 (2011) 2891

Highlights

1. Single-phased nanocrystalline SmB_6 are prepared by a solid-state reaction in a continuous evacuating process.
2. The reaction temperature has a significant effect on the grain size and morphology.
3. The valence state of Sm in nanocrystalline SmB_6 is more likely Sm^{3+}.